JOURNAL OF Applied Polymer SCIENCE

Mechanism of Action of Different *d*-Spacings Clays on the Intumescent fire Retardance of Polymers

Simone Pereira da Silva Ribeiro,[1] Luciana Rocha de Moura Estevão,[2] Celeste Margarida Correia Pereira,[3] Regina Sandra Veiga Nascimento[1]

[1]Instituto de Química, DQO, UFRJ, CT Bloco A, 6° andar, Cidade Universitária, Rio de Janeiro, RJ, CEP: 21941-590, Brazil
[2]Agência Nacional do Petróleo, Gás Natural e Biocombustíveis-ANP, SCM, Av. Rio Branco 65, 17° andar, Centro, Rio de Janeiro, RJ, CEP: 20090-004, Brazil
[3]INEGI, Instituto de Engenharia Mecânica e Gestão Industrial, Rua Doutor Roberto Frias 378, 4200-465 Porto, Portugal
Correspondence to: S. P. da Silva Ribeiro (E-mail: spsilva@iq.ufrj.br)

ABSTRACT: A series of sodic and organophilic clays with different *d*-spacings was added to a polymeric matrix of poly (ethylene-*co*-butyl acrylate) EBA-30, containing an intumescent formulation of ammonium polyphosphate (APP) and pentaerythritol (PER), in order to investigate the influence of the *d*-spacings of the clays on their synergistic effects with the intumescent formulation. A series of samples was evaluated through cone calorimetry, SEM, TG-FTIR, FTIR, and XRD of burned residues. The results revealed that the addition of clays with smaller *d*-spacings led to a synergistic interaction with the intumescent formulation, and consequently to an improvement in the flame retardance of the materials. This effect was not observed with the addition of clays with *d*-spacings larger than 30 Å. For these materials, the formation of a less homogeneous and structured intumescent layer, and a delay in the formation of the phosphocarbonaceous species which act as char precursors was observed. This delay could be responsible for the loss of synergy and also for the type of char morphology formed when larger *d*-spacings clays were used. XRD analyses results indicated that the presence of clays in the materials promoted changes in the crystalline phase of the char when the samples were submitted to higher temperatures. Those changes probably allowed for the maintenance of the structures at high temperatures. © 2013 Wiley Periodicals, Inc. J. Appl. Polym. Sci. 130: 1759–1771, 2013

KEYWORDS: flame retardance; nanostructured polymers; clay; degradation

Received 18 December 2012; accepted 19 March 2013; Published online 6 May 2013
DOI: 10.1002/app.39349

INTRODUCTION

The development of polymeric materials with effective flame retardant properties is becoming more important with time.[1] It has been recognized that the addition of only clay nanoparticles to polymeric matrices does not avoid the complete degradation of the polymer, despite the increase in thermal stability and decrease in the heat release rate registered through the relevant analyses. Furthermore, the exclusive use of clays does not interfere significantly or positively with other important flammability tests results, as for instance LOI (Limit of Oxygen Index) and UL-94, where other factors such as the time for ignition are more determinant.[2] Therefore, the concomitant use of additional fire retardant additives is an important practice, especially if the additive plays a role as a synergic element.

Intumescent formulations are composed of a set of additives which increase the flame retardant properties of polymers. An intumescent formulation is commonly composed of three ingredients: an acid source, a carbonific compound, and a blowing agent. These additives, under heating, form a tumid carbonaceous surface layer, known as "char," which prevents the transfer of heat, fuel, and oxygen, hence ceasing the flame.[3–6] In this study, ammonium polyphosphate (APP) was used as the acid source and blowing agent, and pentaerythritol (PER) was added as the carbonific source.

The sole use of an intumescent formulation rarely leads to suitable LOI results. Therefore, several authors have been searching for additives that could act as synergistic agents. Zeolites, montmorillonite, sepiolite, and even spent catalysts from fluid-bed catalytic cracking units (FCC) in oil refining processes have been reported as synergy agents in fire retardant formulations.[7–12] Our group has observed that both sodic and organophilic clays are able to play this role in a poly[ethylene(30%)–butyl acrylate] copolymer matrix containing an intumescent formulation of APP and PER.[13–15] In addition, it has been observed that the *d*-spacings of clays influence the synergistic effect as well, so that LOI values and UL-94 classification decrease when the *d*-spacings increase.[16]

Therefore, this study aimed to assess, by cone calorimetry analysis, the influence of the *d*-spacings of clays on the fire retardant properties of materials containing an intumescent formulation. An attempt to elucidate this phenomenon was made through the analysis of Scanning Electron Microscopy (SEM) images of the intumescent layer formed, TG-FTIR, FTIR, and XRD of the burned residues.

EXPERIMENTAL

The polymer matrix used was a poly[ethylene(30%)–butyl acrylate] copolymer supplied by Elf-Atochem under the trade name Lotryl 30BA02, hereafter referred to as EBA-30. The intumescent formulation used was composed of ammonium polyphosphate (APP), supplied by Clariant under the trade name of Exolit 422, and pentaerythritol (PER) from Sigma-Aldrich. In the polymeric samples produced, the intumescent formulation represented 30 wt %, with a 3 : 1 ratio of APP : PER where, according to the literature, maximum flame retardancy properties are observed for polyethylene materials.[5] The sodic clay and two organophilic clays studied were supplied by Southern Clays under the trade names Cloisite Na, Cloisite 30B, and Cloisite 15A, respectively. The clays were added to the polymeric mixture in order to account for 3 wt % of the total mass involved. In a previous article, the chemical composition of the sodic clay, the chemical structure of the organic modifiers used in the clay organophilization procedures and the concentrations of these organophilic agents were presented.[16]

The polymers and additives were mixed in a Haake Rheocord 9000 rheometer, equipped with a rheomix chamber 600 and roller blades rotor, at 160°C under 50 rpm for 15 min. The mixture was then pressed at 150°C in a Carver press applying 9000 kgf load on a 10 × 10 cm area to obtain sheets of 3 mm thick, from which all test specimens were obtained.

Cone Calorimetry

Cone Calorimetry was performed using a FTT Thermal Science Stanton Redcroft equipment following the ASTM 1354-04 A standard. The duration of the tests followed the standard recommendation on data collection until 2 min after any flaming or combustion signs cease. Samples measuring 100 × 100 × 3 mm were exposed horizontally to a 50 kW heat flux under irradiation by a conical-shaped radiant electric heater. Each sample was tested in three replicates.

The heat release rate (HRR) is the key parameter obtained by the equipment, although it performs simultaneous acquisition of other complementary data.[2] The other basic data registered by the cone calorimeter along all the burning tests was the sample mass decay, smoke release, and carbon dioxide (CO_2) and carbon monoxide (CO) emissions.

X-Ray Diffraction Analysis (XRD)

X-ray diffraction analysis was carried out in order to measure the *d*-spacings of the clays, before and after processing with the polymer and intumescent additives. The samples were pulverized in a cryogenic mill in order to obtain higher homogenization. Moreover, samples were burned at 280, 350, 430, and 560°C in a furnace under a synthetic air flow and a heating rate of 10°C/min with isotherm of 12 h and analyzed by XRD. This isotherm is important to ensure that all chemical reactions liable to occur at a given temperature took place for char formation. These analyses aimed at identifying possible changes in the crystalline arrangement of the char with the increase of temperature and with the addition of clays with different basal spacings. The analyses were performed in a X-ray diffraction Rigaku Miniflex instrument with a copper anode. Scanning was carried out in a 0.05°/s from 2° to 30° (2θ), using 30 kV and 15 mA voltage and filament current, respectively.

Scanning Electron Microscopy (SEM)

SEM analyses were performed on the intumescent layers formed in the samples, after being analyzed according to UL-94 tests. These analyses were carried out to identify changes in char morphology when clays with different basal spacings were added. The analyses were conducted in a Jeol JSM-6460LV microscope coupled to a Thermo-Noran, Six 200 EDS (Energy Dispersive Spectroscopy) system. A 15 kV operating voltage in a tungsten filament was used, and the images were observed through secondary electrons mode.

TG-FTIR Analysis

Thermogravimetric Analysis (TG) coupled to Fourier Transform Infrared Spectroscopy (FTIR) was carried out to verify whether there were different reactions products formed in the gas phase for the various systems studied. The samples were previously milled in a cryogenic mill to ensure the homogeneity of the material. The analyses were performed in a NETZSCH 209 TG instrument, coupled with the Bruker Vector 22 FTIR spectrometer.

FTIR Residue Analysis

Since the reactions for char formation occur in the condensed phase,[17] a series of FTIR analyses of the residues obtained from heating the samples at different temperatures was carried out. By identifying the reactions taking place in the condensed phase and associating them with the intumescent layer formation, a better understanding of the influence of *d*-spacing of the clays on the synergistic effect could be envisaged.

After processing, the samples were heated in a furnace under air flow, with a heating rate of 10°C/min up to 280, 350, 430, and 560°C, with a final isotherm of 12 h. The analyses were performed using a Nicolet 740 Fourier transform infrared spectrometer and KBr pellets.

RESULTS AND DISCUSSION

d-Spacing Measurements

X-ray Analysis. XRD analyses were performed in order to compare the *d*-spacings of clays before and after processing with the matrix. When the *d*-spacings of clays are kept unchanged after processing with the polymer, it can be considered that a composite was formed. On the other hand, if the *d*-spacings increase, as shown by the peak associated with montmorillonite structure in a diffractogram, an intercalated nanocomposite is liable to have been produced,[2] although a complete characterization of the nanomorphology of the samples requires the combined analysis of XRD patterns and other techniques, especially those involving image generation, such as transmission electron microscopy (TEM) and atomic force microscopy (AFM). Figure

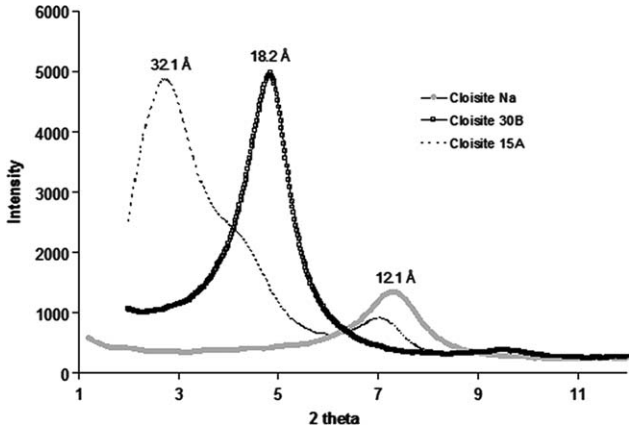

Figure 1. XRD analyses of Cloisites Na, 30B, and 15A.

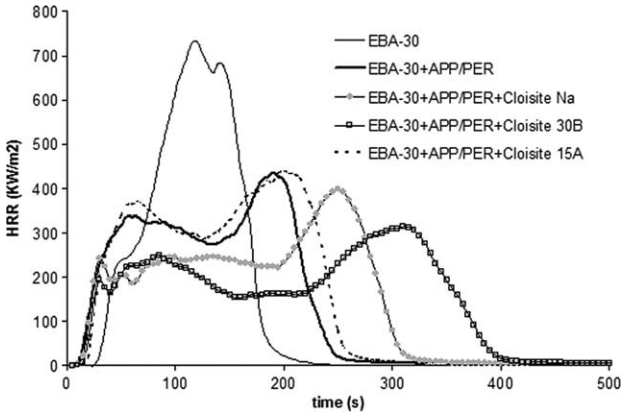

Figure 3. HRR versus Time of the studied materials.

1 presents the diffractograms of clays before processing and the calculated *d*-spacings.

From the results, shown in Figure 2, it is possible to note that there is a small displacement of the Cloisite Na peak after processing, reaching the calculated *d*-spacing around 13.5 Å. However, Cloisites 30B and 15A, respectively presented substantial changes in the displacements towards smaller angles. Cloisite 30B presented an increase in *d*-spacing from 18.2 Å to 21.8 Å after processing. For the Cloisite 15A, the increase was from 32.1 Å to 35.3 Å. These results suggest that the processing of these clays led to the formation of intercalated nanocomposite materials, where clays interacted with the polymeric matrix due to their organophilization. In the case of the sample containing Cloisite Na, the discrete displacement occurred due to the polar characteristic of polymer matrix.

Inflammability Evaluation

Cone Calorimetry. Previous studies[16] have demonstrated that sodic clays with *d*-spacings of up to 24 Å can act as synergistic agents in polymeric materials containing an intumescent formulation when evaluated through LOI. However, when clays with higher *d*-spacings are added, the synergistic effect virtually disappears and the materials cease to classify according to the UL-94 standard.[16] These results have suggested that the clay structure needed to promote synergy disappears with the increase in *d*-spacings, hence reducing the synergistic effect.[16]

In this study, the inflammability of the produced materials is evaluated by cone calorimetry. Figure 3 shows a decrease in the HRR with the addition of the intumescent formulation. The results were also influenced by the *d*-spacings of the added clays. Two peaks are clearly identifiable in the curves of all samples containing the intumescent formulation. The first peak is probably related to the formation of the intumescent layer, whereas the second could be attributed to its degradation.[18] The addition of Cloisites Na and 30B, with *d*-spacings smaller than 24Å, decreased the HRR peaks and delayed the occurrence of the second peak, and hence, char degradation. On the other hand, the addition of Cloisite 15A—with a *d*-spacing larger than 35.3 Å—leads to a slight increase in the HRR, compared to the results obtained for the sample containing only the intumescent formulation. Therefore, according to this technique, the addition of this clay, with a *d*-spacing greater than 30 Å, did not lead to a synergistic effect with the intumescent formulation.

Figure 4 presents the dependence of mass loss of materials with cone calorimetry analysis time. It can be noticed that the addition of the intumescent formulation, despite the clay's *d*-spacing, induces mass loss early on. This phenomenon is related to the formation of the intumescent layer, which is directly linked to the chemical reactions involving the degradation of

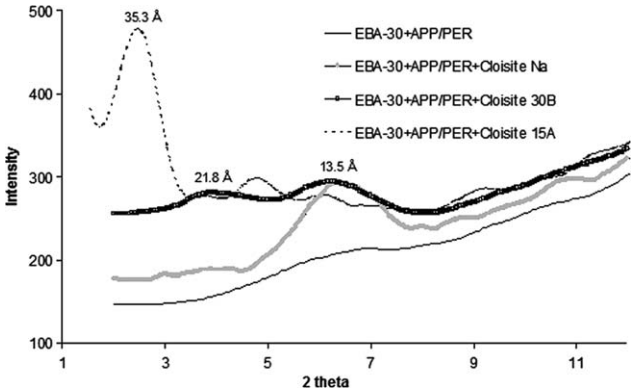

Figure 2. XRD patterns of polymeric samples.

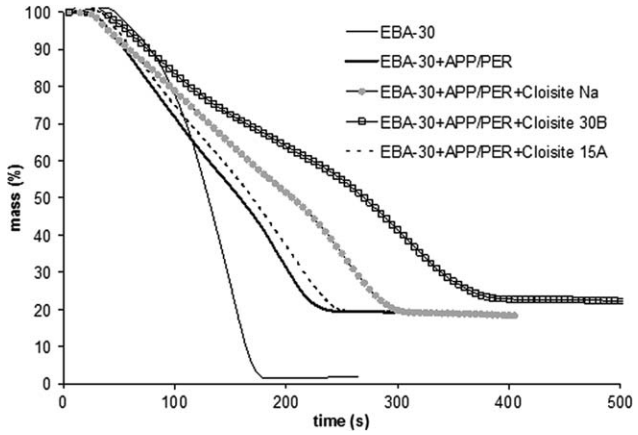

Figure 4. Mass loss over cone calorimetry analysis time.

Table I. Parameters Analyzed by Cone Calorimetry

Sample	THR (kJ)	SEA peak	SEA time to peak (s)	SEA Average (m^2/kg)	CO time to peak (s)	CO average (kg/kg)	CO_2 time to peak (s)	CO_2 average (kg/kg)
EBA-30	899	1316	177	462	220	0.0180	175	1.77
EBA-30 + APP/PER	709	1741	258	796	280	0.0641	260	1.58
EBA-30 + APP/PER + Cloisite Na	683	1346	292	781	335	0.0591	335	1.69
EBA-30 + APP/PER + Cloisite 30B	709	1246	382	787	420	0.0522	380	1.75
EBA-30 + APP/PER + Cloisite 15A	741	1993	277	868	280	0.0648	245	1.73

pentaerythritol, ammonium polyphosphate, and even of the polymeric matrix. In Figure 4, it is possible to observe that the degradation profile of the sample containing only the intumescent formulation (EBA-30 + APP/PER) was not affected by the addition of Cloisite 15A. Also, assigning a defined mass loss, as for instance 60%, the degradation time was virtually the same for both samples. On the other hand, the delay in the degradation for the sample containing Cloisites Na and 30B is evident, indicating the formation of a more effective intumescent layer.

Table I also presents another relevant parameter measured through the cone calorimeter. Besides the aforementioned effect on HRR, the addition of the intumescent formulation decreases the total heat released (THR) of the matrix. The addition of Cloisite Na clay further decreased the THR, when compared to the results obtained for the sample EBA-30 + APP/PER. However, the addition of Cloisite 15A increased it slightly.

The addition of the intumescent formulation increased the amount of smoke produced (SEA, Specific Extinction Area) during burning, as previously observed in other studies.[11] Thus, although the APP/PER system increases the fire resistance of the polymer, once the burning process begins, the mixture containing the formulation releases more smoke than the pure polymer. This is a common disadvantage in the use of intumescent flame retardants. However, the addition of Cloisites Na and 30B decreased the maximum peak of obscuration of the pure polymer, while the addition of Cloisite15A led to a considerable increase of SEA, with a greater peak than that of the sample containing only the intumescent formulation. The same is observed for the SEA average values. Furthermore, the time necessary for the SEA peak to be reached is greater with the intumescent formulation, and is further increased when Cloisites Na and 30B are present. On the other hand, Cloisite 15A decreases this time. These results indicate that the addition of clays with smaller *d*-spacings decreases the obscuration due to smoke production as well as delaying its formation. However, the addition of clay with larger *d*-spacing did lead to worse results in comparison to the EBA-30 + APP/PER sample.

It is noteworthy that it is very important to obtain synergistic agents that reduce the smoke generated and increase its time of appearance in systems containing an intumescent formulation, since obscuring generates panic, causing disorientation of the victims who will have more difficulty to access the emergency exits.

The production of CO and CO_2 is also an important parameter to be measured because these are two gases commonly produced in fires and can cause fatalities. The formation of carbon monoxide is linked to an incomplete combustion, while the carbon dioxide, produced in greater quantity, is related to the complete combustion. Regarding the production of CO, it is observed that the addition of APP–PER increases considerably the formation of this gas. The addition of the Cloisite 30B slightly decreases the concentration of CO, while Cloisite 15A increased the production of CO. Furthermore, the time for the maximum CO peak to be reached is significantly higher than for EBA + APP–PER when Cloisites Na and 30B are added. However, this parameter is unchanged with the addition of Cloisite 15A.

The amount of CO_2 produced stayed practically unchanged when the intumescent formulation and clays were added. However, the maximum concentration of carbon dioxide was reached after a longer period of time when APP–PER was added.

The addition of Cloisites Na and 30B led to yet longer times. However, the presence of the Cloisite 15A decreased the time for the CO_2 peak to be reached, when compared with the sample containing APP/PER only.

Thus, the presence of Cloisite Na and 30B, with *d*-spacings of 13.5 and 21.8 Å respectively, led to an increase in flame retardancy, as measured by cone calorimetry, while the sample containing the Cloisite 15A, with greater *d*-spacing (35.3 Å), showed no improvement over the samples containing only the intumescent formulation. Thus, cone calorimetry also showed that the increase in *d*-spacings leads to a decrease in flame retardance, as previously observed by UL-94 and LOI testing.[16]

Morphology of Char Formed

Scanning Electron Microscopy. Considering the results obtained by cone calorimetry, which show a correlation between the basal spacings of clays and flame retardance, Scanning Electron Microscopy (SEM) was employed to observe the morphology of the char formed with the different clays used. Figure 5 shows SEM images of the char formed upon firing of the samples according to the UL-94 test.

The images show that the pure polymer did not form any type of char, showing a completely smooth surface. Chemical analysis

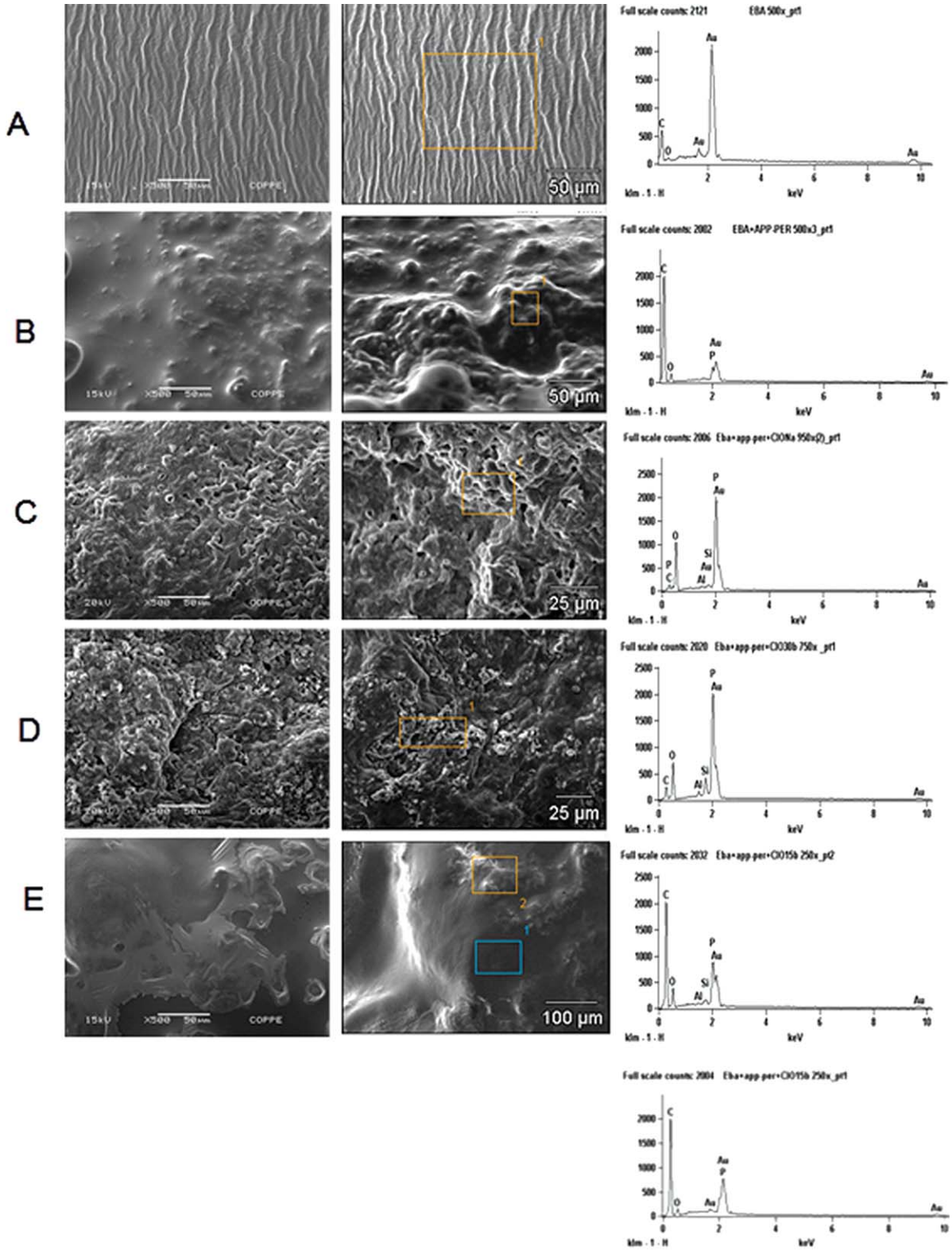

Figure 5. SEM of the char surfaces formed: (A) EBA-30, (B) EBA-30 + APP/PER, (C) EBA-30 + APP/PER + Cloisite Na, (D) EBA-30 + APP/PER + Cloisite 30B, and (E) EBA-30 + APP/PER + Cloisite 15A.[Color figure can be viewed in the online issue, which is available at wileyonlinelibrary.com.]

of this surface revealed the presence of only carbon and oxygen. Sample EBA-30 + APP/PER presented both spongy islands, demonstrating the formation of the intumescent layer, and smooth regions, indicating that the char was not fully formed across the materials surface. Chemical analysis showed the presence of phosphorus in the spongy region, which is characteristic

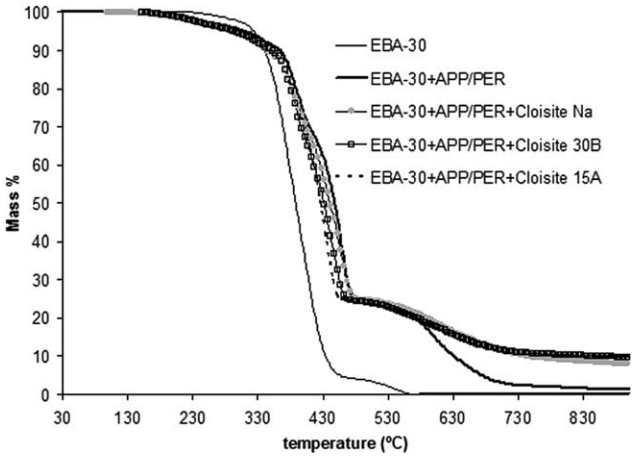

Figure 6. TG curves obtained by TG-FTIR.

of the intumescent layer. However, the addition of Cloisites Na and 30B led to the formation of a more uniform and well-structured intumescent layer which possibly accounts for the enhanced flame retardant properties observed. The chemical analysis results also show the presence of the elements Si and Al, which indicates clay participation in the intumescent layer. Finally, Cloisite 15A which has the largest *d*-spacing, led to the formation of a char with similar morphology to that of the EBA-30 + APP/PER sample, which might explain the low flame retardance properties of the samples containing this clay. Once again the char formed is neither homogeneous nor well structured, alternating smooth and spongy regions similar to those of the sample EBA-30 + APP/PER. The chemical analysis results show the presence of phosphorus, silicon, and aluminum only in the foamed parts. In the smooth regions, only carbon and oxygen were detected as in the pure matrix.

Thus, the addition of clays with various basal spacings induced changes in the morphology of the char formed that influenced the flame retardant properties measured through cone calorimetry.

Understanding the Action of Clays in Synergy

Analysis of the gas phase—TG-FTIR. In order to elucidate the action of clays with different basal spacings on the flame retardance properties of the materials containing the APP/PER formulation TG-FTIR analyses were also performed. This technique was employed in order to investigate whether the clays have any influence on the gas phase reactions. Figure 6 shows the curves obtained through TG.

The thermograms show that the addition of the intumescent formulation increases the degradation temperature compared to that of the pure polymer. Between 220 and 500°C mass losses occur in samples containing APP/PER which are related to char formation reactions. At temperatures below 280°C, a mixture of esters are formed by the reaction of acid species, such as phosphoric acid and orthophosphates generated by the degradation of APP, and the carbonific agent PER. From 280°C on, the carbonization process occurs through the formation of double bonds, generated by the thermal degradation of the esters formed in the previous step, followed by Diels–Alder reactions and free radical processes, which will increase the polyaromatic structure of the char.[19] Between 280°C and 350°C occurs the swelling of the char through the release of ammonia generated from APP degradation.[19] From 500°C to 550°C weight loss decreases and the sample mass is stabilized, indicating the formation of a protective layer which prevents the degradation of the material. However, APP/PER alone does not avoid the complete degradation of the material since at higher temperatures the amount of residue approaches zero. However, the addition of all clays, regardless of their basal spacings, led to an increase in the thermal stability of the char formed, maintaining a residue of about 8% at 900°C. A similar result was obtained in a previous study.[16]

Montmorillonite clays can act as catalysts for various chemical reactions, including Diels–Alder reactions and esterification.[20,21] Thus, sodium and organophilizated clays could favor the reactions that give rise to the polyaromatic structure of the char. The slight decrease of the decomposition temperature with the addition of clays could be an indication of this catalysis. Furthermore, it has been observed that the interlayer spacing of clays have an important role in the catalysis of many chemical reactions. Alkenes, for example, are protonated in the interlayer of clays, being generated carbocation intermediates.[22] In addition, dimerization of unsaturated fatty acids, occurs preferably in the montmorillonite interlayer.[23,24] According to Weiss,[23] the dimerization reaction of oleic acid only occurs because the π bond is in direct contact with the silicate layer of montmorillonite interlayer space, which is probably activated by the empty $3d$ orbital of silicon. Furthermore, compounds such as alcohols and nitriles containing long unsaturated chains, which are arranged in the interlayer space perpendicular or tilted to a large angle, do not dimerize. According to the same author, in these cases, the π connection is far from the silicate layer and cannot be activated. Thus, the increase of the interlayer spacings could hamper the activation of alkenes, leading to a decrease in the reaction rate of formation of polyaromatic hydrocarbons, precursors of char.

From the TG curves, shown in Figure 6, it is not possible to detect differences in the decomposition temperature of the samples containing clays with different basal spacings. However, the addition of all clays, regardless of their basal spacings, led to an increase in the thermal stability of the char formed, maintaining a residue of about 8% at 900°C. A similar result was obtained in a previous study.[15] No significant changes in the decomposition temperatures were detected when using clays with different *d*-spacings.

In order to identify the volatile substances released during the process of thermal decomposition of the materials studied, TG-FTIR analyses were performed. Figure 7 shows the absorbance spectra of the 3D FTIR overheating. The most evident band for all samples appears only at temperatures above 400°C at approximately 2360 cm^{-1} and can be attributed CO_2 molecules.[25] For the samples containing Cloisites 15A and 30B, at 400°C, there is also the appearance of band at 2940 cm^{-1} that is more intense than in the other samples and that is related to the CH_2 groups present in aliphatic hydrocarbons.[25] Although there is some variation in peak intensity, it appears that all

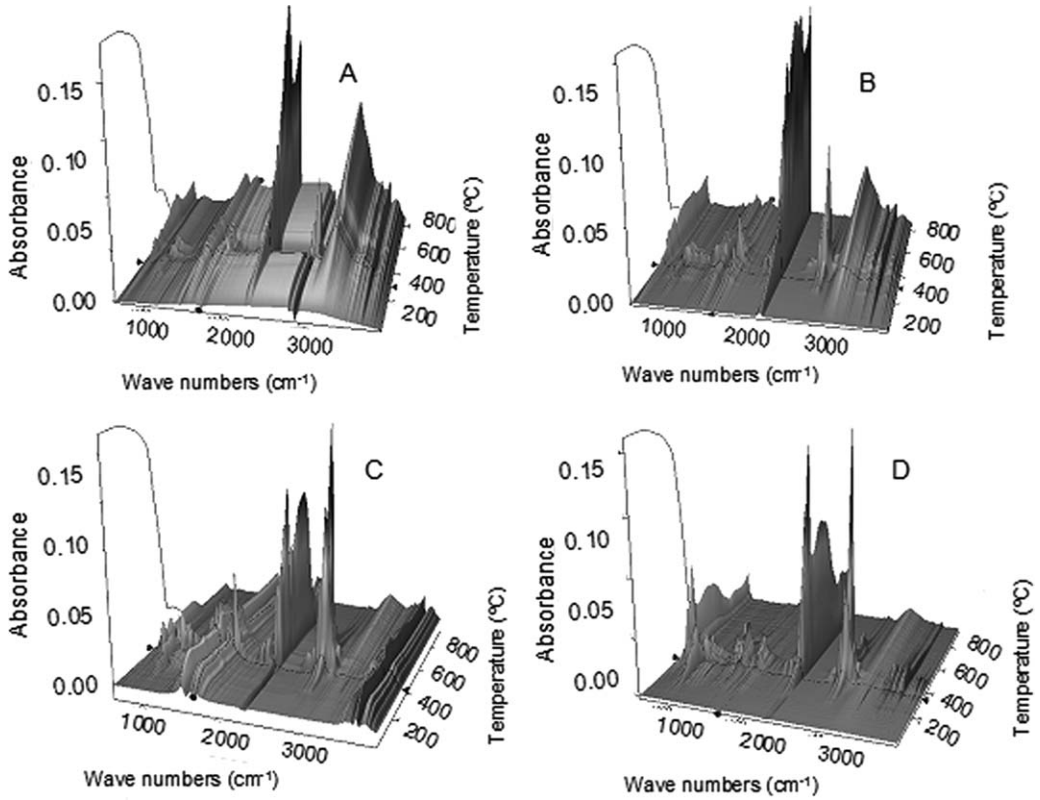

Figure 7. FTIR 3D spectra over temperature: (A) EBA-30 + APP–PER;(B) EBA-30 + APP/PER + Cloisite Na; (C) EBA-30 + APP/PER + Cloisite 30B; and (D) EBA-30 + APP/PER + Cloisite 15A.

samples produced the same bands, indicating no significant differences between the products in the gas phase. Therefore, in principle, the variation of the basal spacings in clays does not influence the formation of volatile products during thermal decomposition, nor gives rise to new reactions at the gas phase. However, for a more detailed analysis, it is necessary to analyze the 2D FTIR spectra obtained at certain temperatures, chosen according to the TG curves in Figure 6. Figure 8 shows the curves of the thermal degradation products at 200, 400, 600, and 800°C, including the temperature ranges where the char is formed (200–400°C), stabilized (600°C), and degraded (800°C).

In Figure 8, there are no significant differences between the spectra of the EBA-30 + APP–PER and clay containing samples, where all samples exhibit very similar bands. The trend observed in 3D graphs (Figure 7) is maintained when analyzed through 2D spectra (Figure 8). Thus, the addition of clay does not seem to lead to significant changes in the formation of volatile products during thermal decomposition, and there is no evidence of new gas phase reactions. Moreover, greater intensities of absorbance are obtained at 400°C, where the char is fully formed, and at 600°C, where its degradation begins, as shown in Figure 6.

Looking in more detail at the spectra obtained (Figure 8), all samples showed bands in the 3700–3900 cm^{-1} region which can be attributed to hydroxyl groups from the water generated by the thermal degradation of [0]the sample, for example.[26,27] A band at 3240 cm^{-1} is evident for all samples and can be correlated with C–H in C=C groups,[26] indicating the formation of unsaturated carbon compounds. Considering that this band is move evident at higher temperatures, it is more likely to derive from the decomposition of the polycondensed aromatic species of the carbonaceous layer than from the formation of unsaturated char precursors.

The bands at 2940, 2865, and 1460 cm^{-1} correspond to the stretching of C–H in CH_2 groups of aliphatic hydrocarbons.[26–28] These compounds can be generated by the degradation of the polymer matrix at 400°C, as shown in Figure 6. The bands at 2360 and 670 cm^{-1} correspond to CO_2 molecules, and the bands at 2180 and 2105 cm^{-1} correspond to CO. For all samples, CO bands have the greatest intensity at 600°C, temperature at which the char is already formed but has not yet degraded, as observed in Figure 6. The presence of CO gas is an indication of incomplete combustion due to the presence of the intumescent layer. The band at 1740 cm^{-1} in the samples containing clay corresponds to C=O stretching and indicates the volatilization of products which contain the carbonyl group of carboxylic acids.[26,27] It is worthwhile to note that the phosphocarbonaceous structures, suggested by Bourbigot et al.[18,29] presented carboxylic acid carbonyl groups attached to polyaromatic structures. The band at 1520 cm^{-1} can be attributed to the angular deformation of the N–H group. Finally, the bands at 965 and 920 cm^{-1} correspond to ammonia molecules generated by the degradation of ammonium polyphosphate and that function as the expansion gas for the intumescent layer. In samples

Applied Polymer SCIENCE

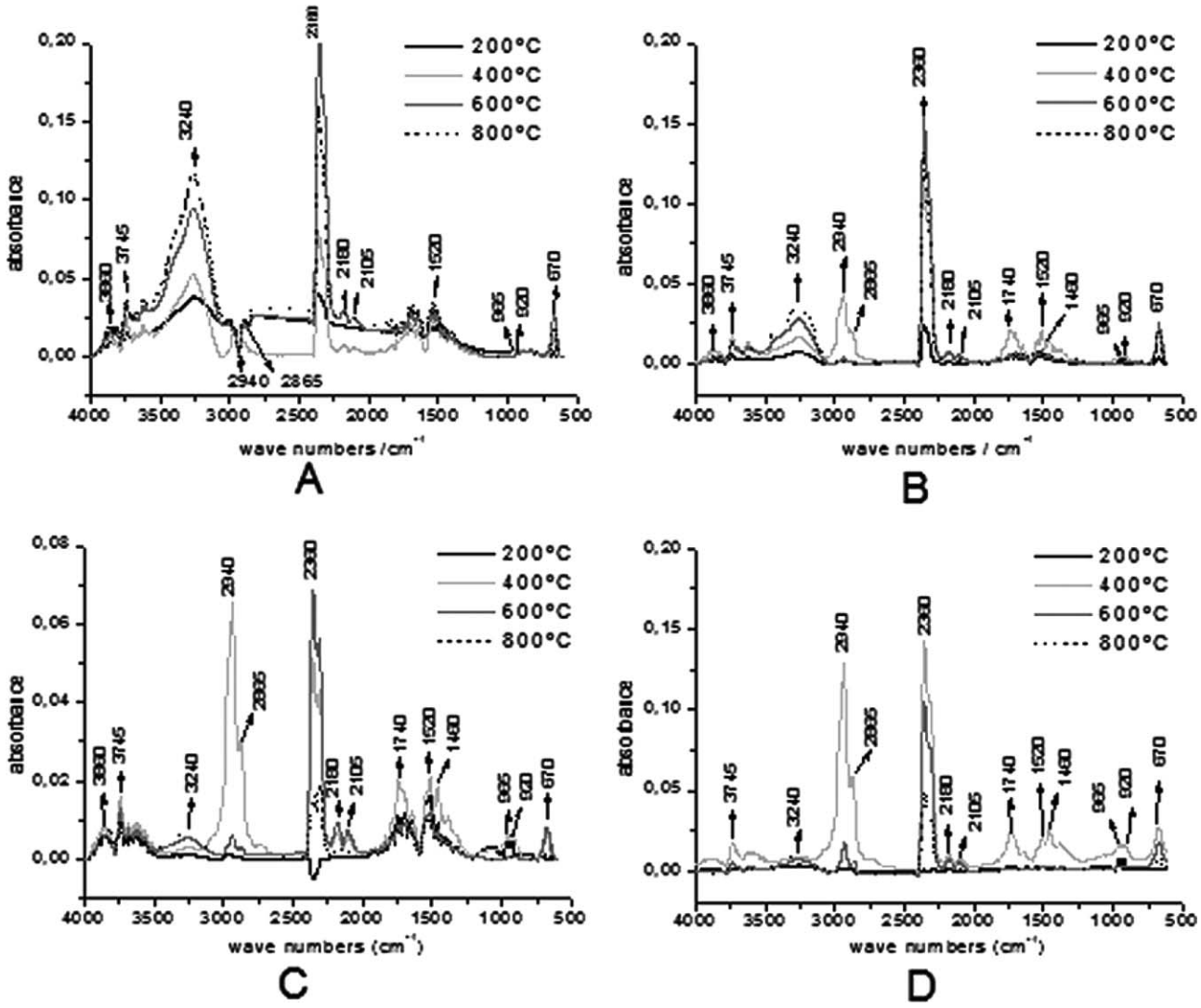

Figure 8. FTIR curves of the thermal degradation products at temperatures 200, 400, 600, and 800°C, obtained by TG-FTIR (A) EBA + APP/PER; (B) EBA + APP/PER + Cloisite Na; (C) EBA + APP/PER + Cloisite 30B; and (D) EBA + APP/PER + Cloisite 15A.

containing organophilic clays, the intensity of these bands is greater, probably due to the quaternary ammonium salts generally used as modifying agents that also release ammonia on thermal degradation.

From Figure 8, it is also possible to verify that there is no involvement of phosphorous groups in the gas phase, since no bands related to the P=O (1268 cm^{-1}) and P–O (1031 cm^{-1}) groups were identified.[26] Thus, the reactions involving the phosphorous groups for the formation of the intumescent layer systems must have all occurred in the condensed phase.

Analysis of the Condensed Phase—FTIR. In order to observe the action of clays with different basal spacings in the condensed phase, mixtures containing these clays and APP/PER in the polymer matrix were analyzed by FTIR before (30°C) and after heating the samples at 280, 350, 430, and 560°C. The spectra obtained are shown in Figure 9.

According to Bourbigot et al.[30] the infrared frequency range of 850–1350 cm^{-1} corresponds to different types of P–O bonds, and allows the characterization of phosphoric species, confirming the presence of a phosphocarbonaceous structure. Another region of interest includes the 2500–3700 cm^{-1} range which corresponds to the absorption of aliphatic groups and allows the observation of the participation of the polymer matrix in the formation of the intumescent layer. Thus, for a better of visualization of the spectra, Figure 9 shows these two bands in the wavelength ranges mentioned above.

Analyzing the first range of 2500–3700 cm^{-1}, two bands are clearly identified at 2850 and 2920 cm^{-1} in all samples at 30, 280, and 350°C. These bands correspond to the symmetrical axial deformation and asymmetrical axial deformation of C–H bonds in polyethylenic chain, respectively.[30–32] The presence of this group provide greater flexibility to the intumescent layer, connecting the polyaromatic structures which are being

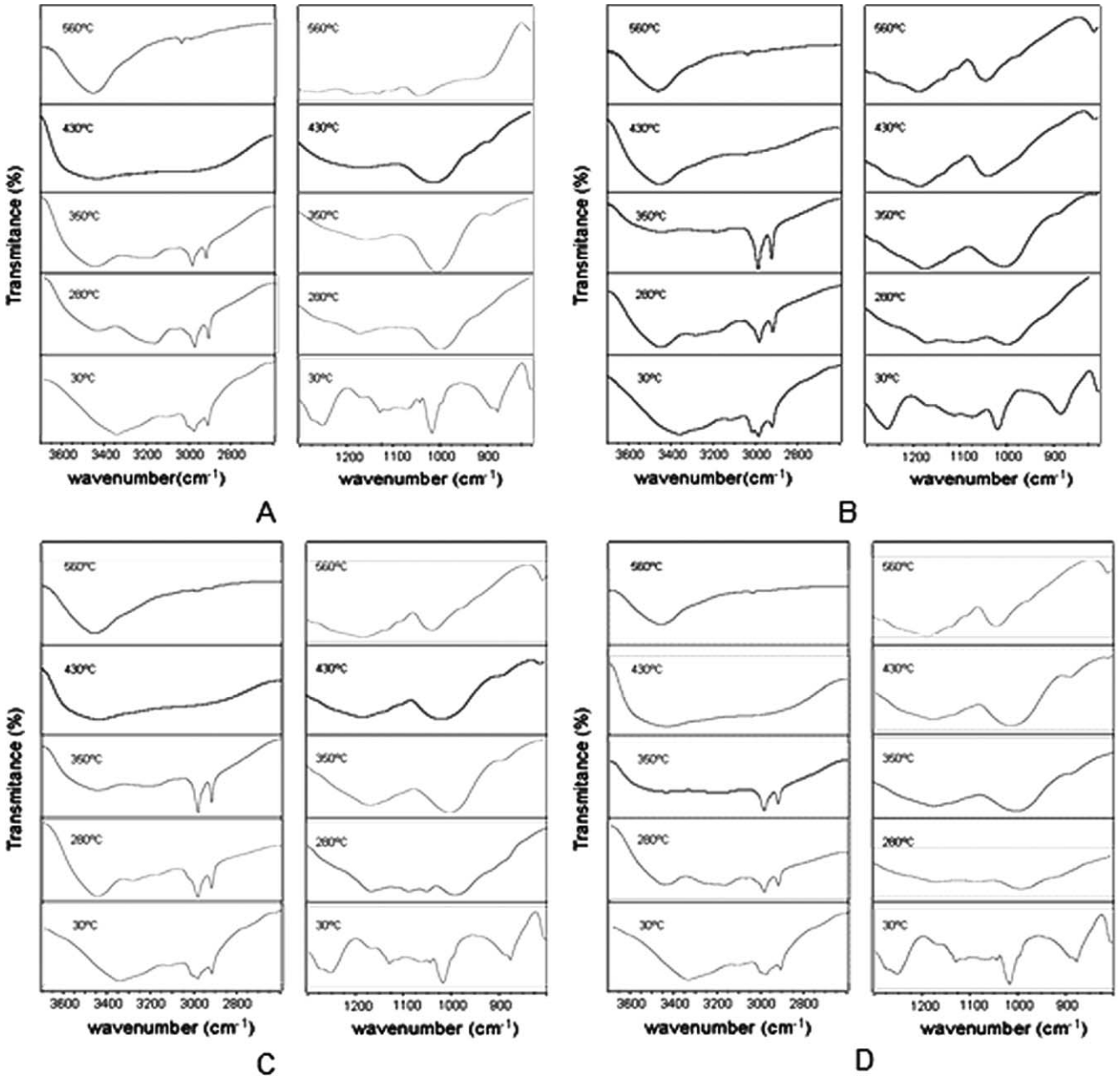

Figure 9. FTIR analyses of the samples produced (30°C) and of their residues of at 280, 350, 430, and 560°C: (A) EBA + APP/PER; (B) EBA + APP/PER + Cloisite Na; (C) EBA + APP/PER + Cloisite 30B; and (D) EBA + APP/PER + Cloisite 15A.

formed.[18,19] A flexible intumescent layer is able to withstand the tensions generated by the release of the gases formed by the burning material, causing a better encapsulation of these gases. However, at 350°C the intensity of these bands is greater for samples containing Cloisites Na and 30B considering the ratio between the bands. The sample containing Cloisite 15A, with higher basal spacing, showed intensities very close to those of the EBA-30 + APP/PER sample. Hence, the presence of greater amounts of these fragments at 350°C suggests that Cloisites Na and 30B may give rise to protective layers with better shielding properties and that are able to retard the degradation of these fragments at higher temperatures.

Analyzing the bands with wavenumbers between 850–1350 cm^{-1}, the 1100–1300 cm^{-1} range shows a band at 1160 cm^{-1} that corresponds to the P–O–C stretching mode in phosphate carbon complexes.[30,32–34] The EBA-30 + APP/PER sample presents this band at 280 and 350°C, but at 560°C, it is no longer observed. Samples containing Cloisites Na and 30B not only presented these bands at 280 to 350°C, but also maintained them at temperatures above 430°C. However, a different behavior was observed in the sample containing Cloisite 15A. In this mixture, the 1160 cm^{-1} band was not present at 280°C, and only became clearly visible at 350°C. Nevertheless, once formed, this band remained identifiable up to 560°C.

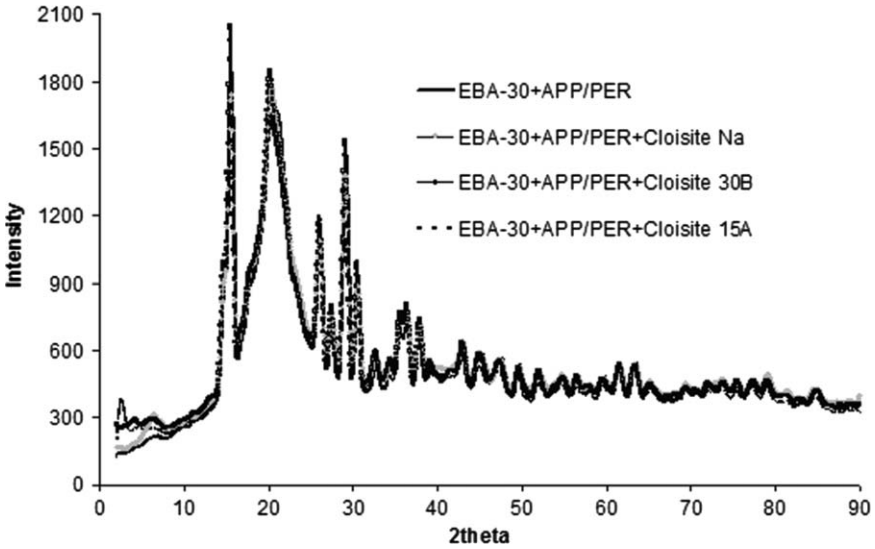

Figure 10. XRD curves of the samples that did not undergo heat treatment (30°C).

FTIR bands in the 980–1020 cm^{-1} range can be observed for all the samples heated from 280 to 560°C, and correspond to the symmetrical axial deformation of PO_2 and PO_3 in complex carbon phosphates.[30]

Analyzing the aforementioned results, it is worth noting that the EBA-30 + APP/PER sample presents no P–O–C bonds at 560°C. This suggests that the layer becomes more rigid by the scission of P–O–C bonds and condensation of the polyaromatic structure. The rigid layer is more brittle and creates cracks on its surface, exposing the material to the flame and permitting its complete degradation. This suggestion is consistent with the TG results shown in Figure 6.

The addition of clays, regardless of their basal spacings, led to the stabilization of the P–O–C bonds up to 560°C. Therefore, the addition of clays prevents the complete scission of the P–O–C bonds, leading to a more flexible intumescent layer. The TG curve shown in Figure 6 indicates that the clays did lead to the formation of a more thermally stable intumescent layer. The possible formation of aluminophosphoric complexes could assist in stabilizing the phosphocarbonaceous structure of the char, therefore increasing its thermal stability.[30,35,36]

However, the addition of Cloisite 15A, which has the largest basal spacing among the clays studied, despite stabilizing the P–O–C bonds to higher temperatures, delayed their formation to 350°C. For all other samples, including the EBA-30 + APP/PER, the 1160 cm^{-1} band was already present at 280°C. This result suggests that increasing the basal spacings of the clays hinders the formation of the phosphocarbonaceous structure that produces char. This hypothesis is consistent with the aforementioned assumption that the greater distance between the silicate layers in the clays could prevent the activation of the π bond for the aromatization reactions that lead to char formation.[19,28,37]

The delay in the formation of the intumescent layer, compared to the other samples, could explain the poor performance of the materials containing Cloisite 15A. Intumescence is a complex process in which all reactions must occur at a specific temperature and time to ensure the formation of a protective shield with optimal properties.[19,37,38] In the process, ester formation and APP decomposition must follow a certain rate in order to produce ammonia at the moment where the carbonaceous structure has adequate properties to withstand swelling.[19,38]

Analysis of the Condensed Phase—XRD. The intumescent layer is a very heterogeneous material, composed of gaseous products stored in the phosphocarbonaceous structure of the condensed phase. This phase is a mixture of liquid (tar) and solid phases, and has dynamic properties that allow the storage of gaseous and liquid products from the degradation of the polymer.[18]

The carbonaceous fraction of the condensed phase consists of polyaromatic species arranged in stacks and the phosphocarbonaceous material consists of macromolecules and crystalline cells of polyaromatic chemical structures connected by polymeric chain fragments and phosphate groups. Besides this crystalline phase, the phosphocarbonaceous material has an amorphous phase surrounding the crystalline domains.[18,38]

This amorphous phase consists of small polyaromatic molecules, alkyl chains formed by the degradation of the additives and polymer chain fragments. This phase must be large enough to completely coat the crystalline domains. Finally, the intumescent layer must have an appropriate balance between stiffness and viscosity that will give the dynamic properties of interest and that will prevent dripping, and also accommodate the tensions generated by solid particles and from the pressure of the gases produced by the burning process[18,38,39]

In order to observe changes in the crystalline phase of the intumescent layer with the addition of clays with various basal spacings, XRD analysis was performed on the samples before and after heating up to 280, 350, 430, and 560°C.

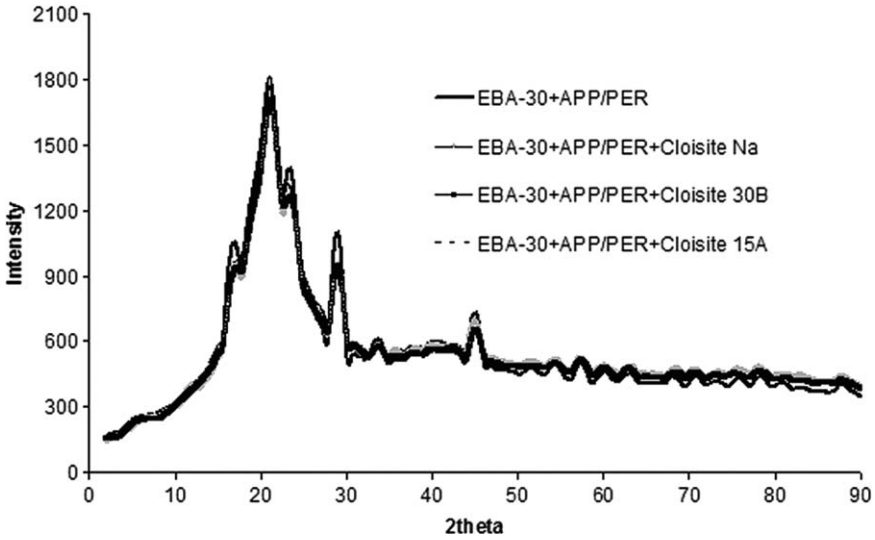

Figure 11. XRD curves of the samples that underwent heat treatment at 280°C.

Figures 10–14 show the XRD patterns obtained for the previously heated samples at 280, 350, 430, and 560°C and that of the non-heated sample (30°C). It can be observed that at 280°C (Figure 11) and 350°C (Figure 12), there is a change in the crystalline structure, since the curve's profiles are different from that of the non-heated sample (Figure 10). This change in the crystalline organization is related to the formation of the intumescent layer. More specifically, it corresponds to crystalline phase changes in the intumescent layer which, as mentioned before, is composed of both an amorphous and a crystalline phase. In this complex medium, crystalline cells of polyaromatic structures are linked together by fragments of polymer chain and by phosphate groups.[18]

Although the diffractogram profiles altered from 280°C to 350°C, indicating changes in the crystalline structure due to temperature, all clay containing samples, regardless of their basal spacing, showed the same profile as the EBA-30 + APP/PER sample at the respective temperatures. Thus, in this temperature range, the addition of clays with various basal spacing does not influence the crystalline structure of the char.

At 430°C (Figure 13), there is a significant decrease in the intensities of the diffraction patterns for all samples. In addition, at this temperature, all clay containing samples showed the same profile. However, this profile differs from that of the EBA-30 + APP/PER sample. These results suggest that temperature increase causes a decrease in the crystalline organization of the structure. Furthermore, in EBA-30 + APP/PER, it appears that the crystalline structure of the phosphocarbonaceous material is destroyed, coinciding with the P–O–C bonds disappearance at this temperature as showed in FTIR analysis [Figure 9(a)]. From these results, it is possible to infer that clay addition preserves the crystalline structure and the P–O–C bonds at this

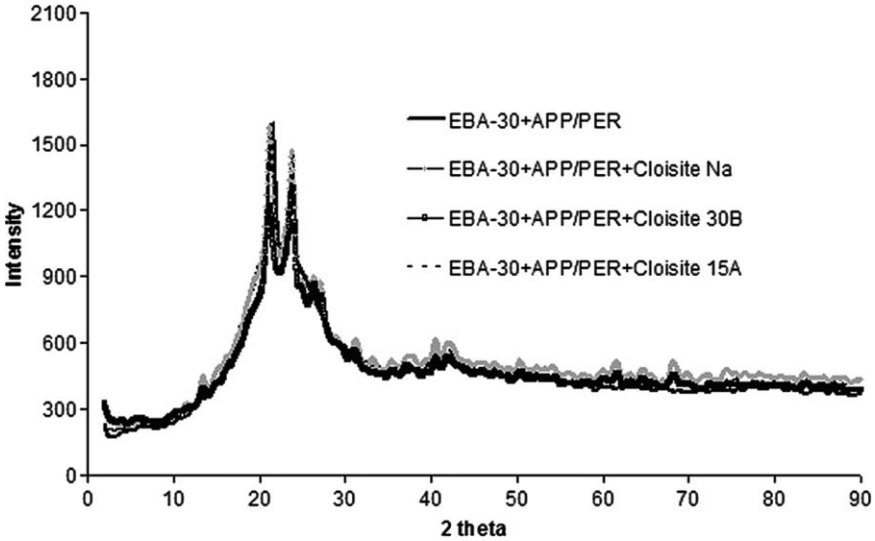

Figure 12. XRD curves of the samples that underwent heat treatment at 350°C.

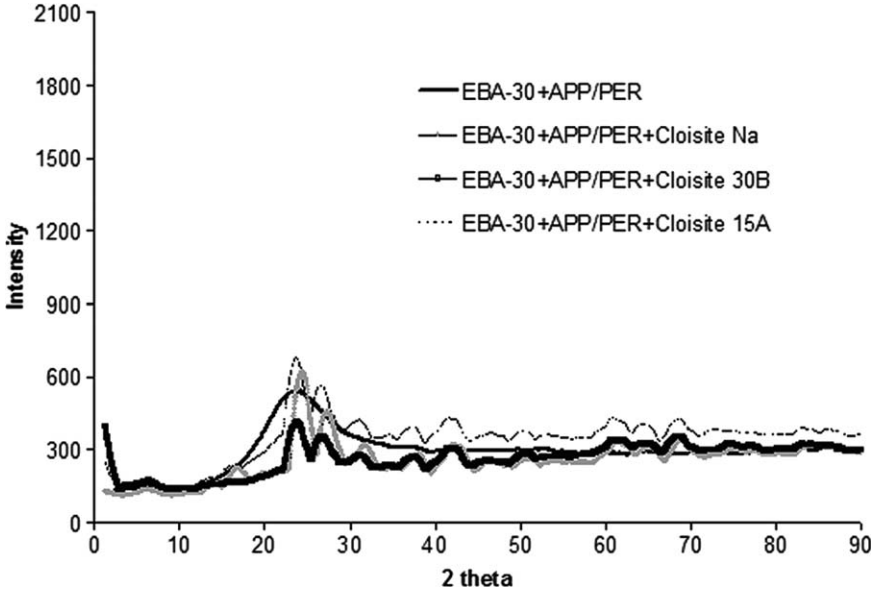

Figure 13. XRD curves of the samples that underwent heat treatment at 430°C.

temperature [Figure 9(B–D)]. No significant differences were observed regarding the basal spacing of the clays studied.

Figure 14 shows a significant increase in peak intensities at 560°C for the samples containing clays, whereas the EBA-30 + APP/PER peaks did not undergo this increase. Once again, the diffraction patterns observed for all clay containing samples were very similar, regardless of the basal spacing of the clays, but differed from that of the sample without the clay. These results indicate that the presence of the clays lead to a more organized crystalline phase, but the presence of P–O–C bonds, still detected at 560°C [Figure 9(B–D)] confers flexibility to the protective layer and stabilizes it at high temperatures. [0]Yet again, no differences were observed in the crystalline structure in relation to the basal spacings of the clays used. Bourbigot et al.[30] in studying an ethylenic terpolymer containing APP/PER and zeolite 4A by Nuclear Magnetic Resonance (NMR) of Al^{27}, Si^{29}, and P^{31}, observed an increase in the thermal stability of the char formed with the zeolite, and attributed this effect to the formation of organic aluminosilicophosphate complex during burning. The production of these species would reduce the scission of P–O–C bonds and therefore the increase in the size of polyaromatic stacks. This fact would justify the increase of the organization of the crystalline structure in samples with clays and submitted to 560°C. The aluminophosphate species could also increases the efficiency of the intumescent char shield.[40]

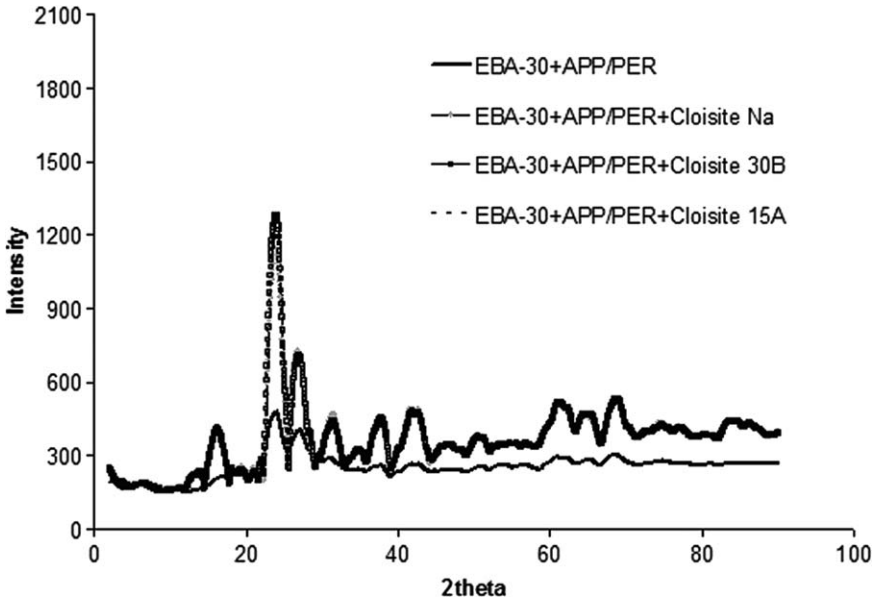

Figure 14. XRD curves of the samples that underwent heat treatment at 560°C.

CONCLUSIONS

Cone calorimetry revealed that the addition of clays with basal spacings greater than 30 Å for materials containing an EBA-30 matrix and an APP/PER intumescent formulation lead to a loss of the synergistic action obtained with clays with smaller basal spacings, such as 13 and 22 Å.

The SEM analysis results showed that the addition of Cloisite 15A with a basal spacing greater than 30 Å, led to the formation of an intumescent layer with a morphology very similar to the one of the sample containing only APP–PER. These layers are less homogeneous and structured than those containing clays with basal spacings of 13 or 22 Å.

The results of the TG-FTIR analysis suggest that clays act exclusively in reactions taking place in the condensed phase. The FTIR analyses of the residues obtained from the heating treatments employed indicate a delay in the formation of the phosphocarbonaceous species when clays with larger basal spacings are added. This effect can justify the loss of synergy and the differences in morphology of the char formed.

Finally, XRD results indicate that the presence of clays in the materials promoted changes in the crystalline phase of the char when the samples were submitted to temperature increase. Those changes allowed for the maintenance of the structures at higher temperatures.

REFERENCES

1. Laoutid, F.; Bonnaud, L.; Alexandre, M.; Lopez-Cuesta, J. M.; Dubois, Ph. *Mater. Sci. Eng. R. Rep.* **2009**, *63*, 100.
2. Kiliares, P.; Papaspyrides, C. D. *Prog. Polym. Sci.* **2010**, *35*, 902.
3. Jimenez, M.; Duquesne, S.; Bourbigot, S. *Surf. Coat. Technol.* **2006**, *201*, 979.
4. Le Bras, M.; Bourbigot, S. In Fire Retardancy of Polymers: The Use of Intumescence; Le Bras, M., Camino, G., Bourbigot, S., Delobel, R., Eds.; The Royal Society of Chemistry: London, **1998**; Chapter 3, pp 64–75
5. Bourbigot, S.; Le Bras, M.; Bréant, P.; Trémillon, J. M.; Delobel, R. *Fire Mater.* **1996**, *20*, 145.
6. Bourbigot, S.; Le Bras, M.; In Fire Retardancy of Polymers: The Use of Intumescence; Le Bras, M., Camino, G., Bourbigot, S., Delobel, R., Eds.; The Royal Society of Chemistry: London, **1998**; Chapter 13, pp 222–235.
7. Shumao, L.; Hua, Y.; Tao, Y.; Weizhong, Y.; Jie, R. *Polym. Adv. Techol.* **2009**, *20*, 1114.
8. Yun, L.; Jun-Sheng, W.; Cheng-Liang, D.; De-Yi, W.; Yan-Peng, S.; Yu-Zhong, W. *Polym. Adv. Techol.* **2010**, *21*, 789.
9. Estevão, L. R. M.; Nascimento, R. S. V.; Le Bras, M.; Delobel, R. In Fire Retardancy of Polymers New Application on Mineral Fillers; LeBras, M., Wilkie, C. A., Bourbigot, S., Duquesne, S., Jama, C., Eds.; The Royal Society of Chemistry: Cambridge, **2005**; Chapter 23, pp 313–326.
10. Estevão, L. R. M.; Nascimento, R. S. V. *Polym. Degrad. Stab.* **2002**,*75*, 517.
11. Estevão, L. R. M.; Le Bras, M.; Delobel, R.; Nascimento, R. S. V. *Polym. Degrad. Stab.* **2005**, *88*, 444.
12. Huang, N. H.; Chen, Z. J.; Wang, J. Q.; Wei, P. *Express. Polym. Lett.* **2010**, *4*, 743.
13. Ribeiro, S. P. S.; Estevão, L. R. M.; Nascimento, R. S. V. *J. Therm. Anal. Calorim.* **2007**, *87*, 661.
14. Ribeiro, S. P. S.; Estevão, L. R. M.; Pereira, C.; Rodrigues, J.; Nascimento, R. S. V. *Polym. Degrad. Stab.* **2008**, *94*, 421.
15. Ribeiro, S. P. S.; Estevão, L. R. M.; Csaba, N.; Nascimento, R. S. V. *J. Therm. Anal. Calorim.* **2011**, *106*, 535.
16. Ribeiro, S. P. S.; Estevão, L. R. M.; Nascimento, R. S. V. *Sci. Technol. Adv. Mater.* **2008**, 9, doi:10.1088/1468-6996/9/2/024408.
17. Lewin M. In Fire Retardancy of Polymers: The Use of Intumescence; Le Bras, M., Camino, G., Bourbigot, S., Delobel, R., Eds.; The Royal Society of Chemistry: London, **1998**; Chapter 1, pp 3–32.
18. Bourbigot, S.; Duquesne, S. In Flame Retardant Polymer Nanocomposites Intumescence and Nanocomposites; Morgan, A. R., Wilkie, C. A., Eds.; Wiley: New Jersey, **2007**; Chapter 6, pp 131–162.
19. Bourbigot, S.; Duquesne, S. *J. Mater. Chem.* **2007**, *17*, 2283.
20. Soma, Y.; Soma, M. *Environ. Health Perspect.* **1989**, *83*, 205.
21. Adams, J. M.; Dyer, S.; Martin, K.; Matear, A.; McCabe, R. W. *J. Chem. Soc. Perkin Trans.* **1994**, *1*, 761.
22. Laszlo, P. *Science* **1987**, *235*, 1473.
23. Weiss, A. *Angew. Chem. Int. Ed. Engl.* **1981**, *20*, 850.
24. Koster, R. M.; Borget, M.; de Leeuw, B.; Poels, E. K.; Bliek, A. *J. Mol. Catal. A: Chem.* **1998**,*134*, 159.
25. Miller, T. W. *J. Therm. Anal. Calorim.* **2011**, *106*, 249.
26. Yi, L.; Jiang Song, Y.; Xufu, C. *J. Therm. Anal. Calorim.* **2012**, *107*, 1191.
27. Wang, K.; Lv, P.; Hu, Y.; Hu, K. *J. Anal. Appl. Pyrol.* **2009**, *86*, 207.
28. Herrera, M.; Mattuschek, G.; Kettrup, A. *J. Therm. Anal. Calorim.* **2000**, *59*, 385.
29. Bourbigot, S.; Le Bras, M.; Delobel, R. *Carbon* **1993**, *31*, 1219.
30. Bourbigot, S.; Le Bras, M.; Delobel, R. *J. Chem. Soc. Faraday Trans.* **1996**, *92*, 3435.
31. Liu, W.; Chen, D.-Q.; Wang, Y.-Z.; Wang, D.-Y.; Ming-Hai, Q. *Polym. Degrad. Stab.* **2007**, *92*, 1046.
32. Le Bras, M.; Bourbigot, S.; Revel, B. *J. Mater. Sci.* **1999**, *34*, 5777.
33. Thomas, L. C.; Chittenden, R. A. *Spectrochim. Acta* **1964**, *20*, 489.
34. Yi, J.; Liu, Y.; Pan, D.; Xufu, C.. *J. Appl. Polym. Sci.* **2012**, *127*, 1061.
35. Tang, Y.; Hu, Y.; Li, B.; Liu, L.; Wang, Z.; Chen, Z.; *J. Polym. Sci. Part A: Polym. Chem.* **2004**, *42*, 6163.
36. Tang, Y.; Hu, Y.; Wang, S.; Gui, Z.; Chen, Z. *Polym. Int.* **2003**, *5*, 1396.
37. Antonov, A. V. *Russ. Chem. Rev.* **1999**, *68*, 605.
38. Wei, P.; Hao, J.; Du, J.; Han, Z.; Wang, J. *J. Fire Sci.* **2003**, *21*, 17.
39. Shartel, B.; Wei, A.; Mohr, F.; Kleemeier, M.; Hartwig, A.; Braun, U. *J. Appl. Polym. Sci.* **2010**, *118*, 1134.
40. Chen, Y.; Fang, Z.; Yang, C.; Wang, Y.; Guo, Z.; Zhang, Y. *J. Appl. Polym. Sci.* **2010**, *115*, 777.